2019

Investigation of the Cofiring Process of Raw or Torrefied Bamboo and Masson Pine by Using a Cone Calorimeter

Hongzhong Xiang

Jianfei Yang

Zixing Feng

Wanhe Hu

Fang Liang

See next page for additional authors

Authors

Hongzhong Xiang, Jianfei Yang, Zixing Feng, Wanhe Hu, Fang Liang, Liangmeng Ni, Qi Gao, and Zhijia Liu

ACS OMEGA

Article

Cite This: ACS Omega 2019, 4, 19246−19254

http://pubs.acs.org/journal/acsodf

Investigation of the Cofiring Process of Raw or Torrefied Bamboo and Masson Pine by Using a Cone Calorimeter

Hongzhong Xiang,[†,‡] Jianfei Yang,[†,‡] Zixing Feng,[†,‡] Wanhe Hu,[§] Fang Liang,[†,‡] Liangmeng Ni,[†,‡] Qi Gao,[†,‡] and Zhijia Liu*[,†,‡]

[†]International Centre for Bamboo and Rattan, Beijing 100102, Beijing, China

[‡]SFA/Beijing Key Lab of Bamboo and Rattan Science and Technology, Beijing 100102, Beijing, China

[§]School of Natural Resources, West Virginia University, Morgantown 26506, West Virginia, United States

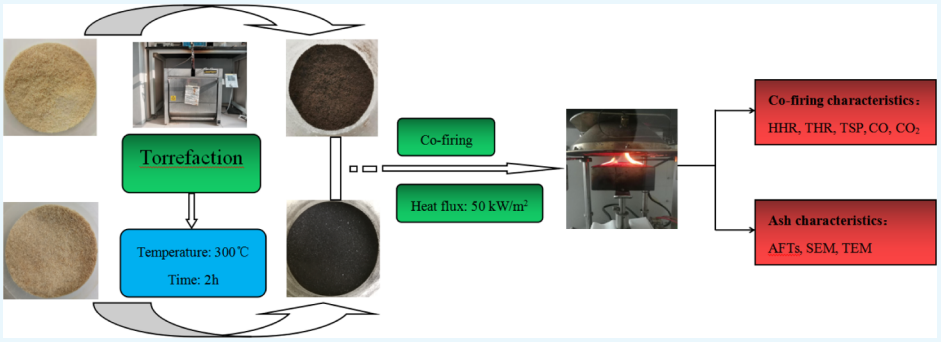

ABSTRACT: Cofiring characteristics of raw or torrefied bamboo and masson pine blends with different blend ratios were investigated by cone calorimetry, and its ash performance from cofiring was also determined by a YX-HRD testing instrument, X-ray fluorescence, scanning electron microscopy (SEM), and transmission electron microscopy (TEM). Results showed that bamboo and masson pine had the different physicochemical properties. Torrefaction improved fuel performances, resulting in a more stable cofiring process. It also decreased the heat release rate, total heat release, and total suspended particulates of fuels, especially CO_2 and CO release. Masson pine ash mainly included CaO, SiO_2, Fe_2O_3, K_2O, and Al_2O_3. Bamboo ash was mainly composed of K_2O, SiO_2, MgO, and SO_3. There were different melting temperatures and trends between different samples. The synergistic reaction of ash components was found during the cofiring process. The surface morphology of blend ash changed with the variation of bamboo or masson pine content.

1. INTRODUCTION

Cofiring technology is widely regarded as a promising way to use biomass as a solid fuel with some advantages such as improving combustion efficiency and reducing pollutant emissions, and so forth. Cofiring of waste biomass and coal could improve ignition and carbon combustion properties of coal.[1] Cofiring wood and wheat straw pellets could improve the thermal decomposition of blends and combustion of volatiles.[2] Tokarski et al.[3] concluded that cofiring of biomass fuels had the minimum energy consumption and the maximum efficiency of power generation, compared with individual combustion of biomass. Furthermore, the release of main nitrogenous gases (HCN, NH_3, NO, and HNCO) also decreased in different blends of biomass (corn straw, cotton stalk, and wheat straw) with municipal sewage sludge during the cofiring process.[4] Kwong et al.[5] confirmed that gaseous pollutant emissions including carbon monoxide (CO), carbon dioxide (CO_2), nitrogen oxides (NO_x), and sulfur dioxide (SO_2) decreased when bamboo was added to coal. Therefore, cofiring technology could improve combustion characteristic of fuels and provide a better control of emissions with some economic benefits.

Bamboo is a type of biomass resource with great potential to be used as a solid fuel because of fast growth, low ash content, alkali index (AI), and heating value. Similar to other biomass, bamboo also has some disadvantages to limit its energy application, such as a low energy density, a high moisture content, a high value of collection, storage and transportation, and so forth. Torrefaction is considered as a good technology to solve these problems. Bamboo underwent chemical changes related to carbonyl groups, mostly present in hemicelluloses, and to aromatic groups present in lignin during the torrefaction process.[6] The calorific value of bamboo also increased from 17.60 to 23 and 28 MJ/kg when it was torrefied at a temperature of 250 and 380 °C.[7] Liu et al.[8] concluded that the presence of bamboo and torrefied bamboo improved the thermochemical reactivity of bamboo and coal blends during the cofiring process. Mi et al.[9] found that the cofiring process of torrefied bamboo, torrefied wood, and their blends included drying, oxidative pyrolysis, and char combustion. Cone

Received: August 13, 2019
Accepted: October 25, 2019
Published: November 4, 2019

DOI: 10.1021/acsomega.9b02593
ACS Omega 2019, 4, 19246−19254

Table 1. Physico-Chemical Characteristics of Samples[a]

samples	proximate analysis (%)				ultimate analysis (%)					HHV (MJ/kg)
	ash	volatiles	FC	moisture	C	H	N	S	O	
masson pine (M)	0.56	84.24	15.21	10.08	51.55	5.36	0.06	0.02	43.01	18.20
bamboo (B)	0.87	81.95	15.20	6.45	49.53	5.62	0.14	0.03	44.68	18.70
torrefied masson pine (TM)	0.64	56.19	43.18	3.29	67.51	4.59	0.06	0.01	27.83	25.92
torrefied bamboo (TB)	1.11	54.13	44.58	0.83	65.65	4.92	0.24	0.03	29.16	25.47
20B:80M	0.53	84.18	15.31	9.80	51.00	5.31	0.02	0.02	43.65	18.65
40B:60M	0.52	84.14	15.34	9.00	50.91	5.41	0.07	0.02	43.59	18.62
60B:40M	0.47	83.93	15.61	8.15	50.78	5.44	0.09	0.03	43.66	18.64
80B:20M	0.46	84.08	15.46	7.38	49.53	5.57	0.16	0.03	44.71	18.61
20TB:80TM	0.75	55.36	43.89	3.40	66.72	4.92	0.18	0.02	27.83	25.30
40TB:60TM	0.83	54.28	44.89	3.57	66.74	4.93	0.24	0.02	28.07	25.51
60TB:40TM	0.92	54.12	44.96	3.72	66.21	4.94	0.26	0.02	28.57	25.52
80TB:20TM	0.98	53.66	45.37	3.74	66.75	5.00	0.27	0.02	27.96	25.56

[a]FC is fixed carbon, HHV is the higher heating value.

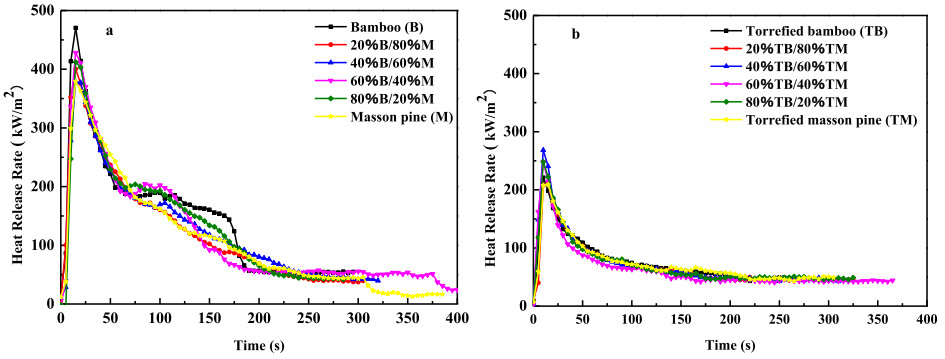

Figure 1. HRR curves of all the samples (a) raw bamboo and masson pine; (b) torrefied bamboo and masson pine.

calorimetry has been widely used to determine flame retardant properties of materials.[10] It can comprehensively evaluate combustion characteristics based on these parameters including heat release rate, total heat release (THR), time to ignition, mass loss rate, total suspended particulates (TSP), specific extinction area, effective heat of combustion, and the yield of CO and CO_2. Our group published the cofiring characteristics of raw/torrefied bamboo and masson pine or coal using thermogravimetric analysis. To the best of our knowledge, there is a lack of sufficient information concerning the cofiring characteristics of bamboo and masson pine by using cone calorimetry. The combustion characteristics from cone calorimetry is very helpful to further comprehensively evaluate cofiring characteristics of bamboo and masson pine. Therefore, raw or torrefied bamboo and masson pine were, respectively, mixed with different blend ratios of 20:80, 40:60, 60:40, and 80:20. Combustion performance of the blends were determined by cone calorimetry at a heat flux of 50 kW/m^2. Ash characteristics from the cofiring process of bamboo and masson pine were also investigated by X-ray fluorescence (XRF), a YX-HRD testing instrument, SEM, and TEM. The results from this research will further develop bamboo and masson pine residues to be used as solid fuels.

2. RESULTS AND DISCUSSION

2.1. Physico-Chemical Characteristics of Blends. The proximate and ultimate analysis and the high heating value of samples are showed in Table 1. The physico-chemical properties of bamboo were similar to those of masson pine, even though bamboo had a slightly high content of ash, hydrogen, nitrogen, sulfur, oxygen, and higher heating value (HHV). Torrefaction improved the fuel properties of bamboo and masson pine, increasing fixed carbon (FC), carbon content, HHV, and decreasing volatiles, moisture, and oxygen. This was attributed to the decarboxylation of biomass in the process of torrefaction, releasing in the form of water, carbon dioxide, carbon monoxide, and oxygen-containing carbohydrates.[11] Furthermore, a decrease in the moisture content of torrefied masson pine and bamboo was beneficial for the fuel to be more easily ignited and to reach higher temperatures.[12] The HHV of masson pine and bamboo, respectively, increased from 18.20 to 25.92 MJ/kg and from 18.70 to 25.47 MJ/kg after they were torrefied. Chen et al.[13] found that carbon, hydrogen, or FC were the primary sources of HHV by calculating correlations in terms of proximate, elemental, or fiber analysis. The HHV increase of torrefied masson pine and bamboo was mainly because of the increase of carbon (from 51.55 and 49.53 to 67.51 and 65.65%, respectively) and FC (from 15.21 and 15.20 to 43.18 and 44.58%, respectively). Ash, moisture, and carbon content of the samples had a slight decrease with the increase of bamboo content in blends. In contrast, the content of FC, carbon, and HHV significantly increased. Compared with raw biomass, the content of ash, FC, moisture, hydrogen, nitrogen, and HHV increased with the increase of torrefied bamboo content in the blends. Furthermore, the effect of blend ratios on the proximate and ultimate analysis of bamboo and masson pine blends was more significant than that of torrefied biomass blends. This confirmed that torrefaction improved fuel properties, resulting in them having more similar physico-chemical performance.

DOI: 10.1021/acsomega.9b02593
ACS Omega 2019, 4, 19246−19254

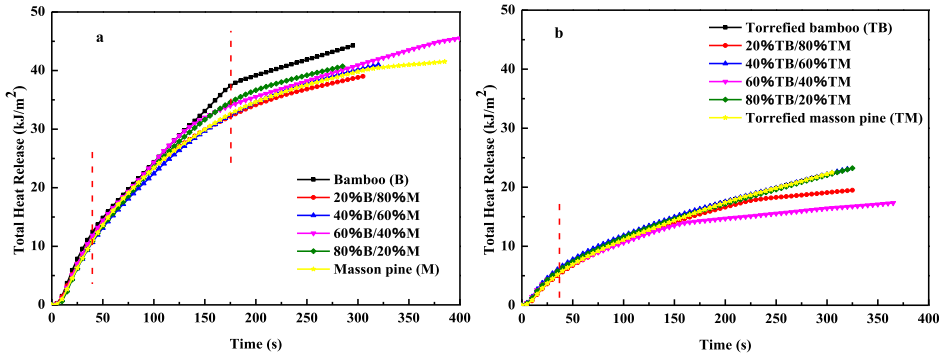

Figure 2. THR curves of all the samples (a) raw bamboo and masson pine; (b) torrefied bamboo and masson pine.

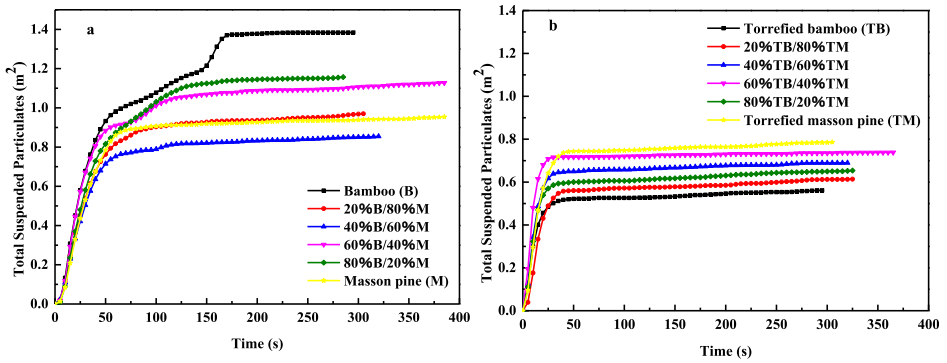

Figure 3. TSP curves of all the samples (a) raw bamboo and masson pine; (b) torrefied bamboo and masson pine.

2.2. Cofiring Characteristics. HRR is the rate of heat release per unit area of the burning sample, which is considered as the most important parameter to characterize the flame strength. Figure 1 shows the HRR curves of the cofiring process for raw and torrefied bamboo and masson pine. There are two distinct release peaks for the cofiring process of raw bamboo and masson pine. But only one peak was found during the cofiring process of torrefied bamboo and masson pine. The first peak corresponds to the maximum value of HRR, which is called as the peak heat release rate (PHRR). The PHRR from the cofiring process of raw biomass was obviously higher than that of the torrefied biomass, which was attributed to the heat release of volatile combustion. Table 1 confirms that all blends of raw biomass had a higher volatile content than the torrefied biomass. Furthermore, the blends of the torrefied biomass had a lower volatile fuel ratio [VM/(VM + FC)] than the blends of raw bamboo or masson pine. This indicated that the blends of torrefied bamboo and masson pine had a lower thermal reactivity and higher ignition temperature because a lot of flammable volatiles were pyrolyzed during the torrefaction process.[14] The values of the first exothermic peak were 378.6–470.4 kW/m^2 for raw biomass blends under different blend ratios, which were also obviously higher than that of the blends of the torrefied biomass. And the second peaks of the blends of raw biomass were broad peaks with values of 160.4 and 202.4 kW/m^2. The second exothermic peak was because of the formation of a protective carbon layer during the combustion process.[15] The samples under the carbon layer were burned because of higher volatile content, which formed the second peak.[16] Compared with the cofiring process of raw biomass, torrefied biomass with different blend ratios had a more stable combustion process. This indicated that torrefaction improved the combustion properties, which can convert bamboo and masson pine with nonuniform qualities into a highly homogenous solid fuel.

Figure 2 shows THR curves of the cofiring process. THR is the total amount of heat released per unit area of the material during the combustion process. The combination of HRR and THR can be used to evaluate the combustion characteristics of a material. There were three stages during the cofiring process of raw biomass. The THR rapidly increased at the first stage corresponding to the first peak of HHR because volatiles from the surface of the samples were ignited. The second stage corresponded to the second peak of HHR, which had a slightly slower THR than the first stage. The carbon layer on the surface of the samples hindered oxygen or air entry, resulting in slower combustion of the samples. The third stage had the slowest THR because of char burning. This also confirmed that flame combustion had a faster THR than char burning during the cofiring process of raw biomass. The cofiring process of torrefied biomass had two burning stages. The first stage with relatively rapid THR was flame combustion. Then char burning also resulted in a stable increase of THR. It was further confirmed that the exothermic stability of the samples was improved after torrefaction.

The exhaust gas emission-related parameters are also an important index to evaluate the combustion properties of fuels. Figure 3 shows the TSP of the cofiring process. For blends of raw biomass, there were three stages of TSP, respectively, corresponding to THR. Similarly, the blends of torrefied biomass had two stages of TSP. Furthermore, the TSP of all the blends rapidly increased at the flaming combustion stage, where the smoke contained a large amount of incombustible volatiles. It was also obvious that the blends of raw biomass had more TSP than the blends of torrefied biomass. Some organic substances were not completely oxidized because of

DOI: 10.1021/acsomega.9b02593
ACS Omega 2019, 4, 19246−19254

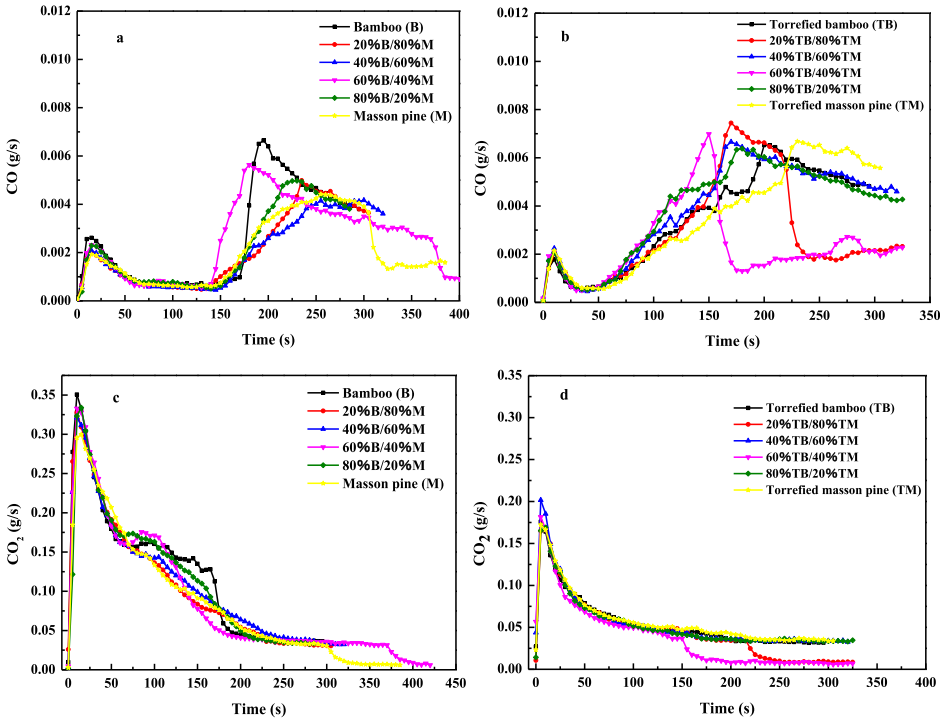

Figure 4. CO and CO_2 curves of all the samples (a) CO release from raw bamboo and masson pine; (b) CO release from torrefied bamboo and masson pine; (c) CO_2 release from raw bamboo and masson pine; (d) CO_2 release from torrefied bamboo and masson pine.

low combustion temperatures, which promoted smoke release. This phenomenon was related to the moisture content and volatiles of the samples. Hellwig[17] concluded that high water content of biomass materials could lead to poor ignition. Table 1 confirms that raw biomass also had a higher moisture content, resulting in fuels that were more difficult to be ignited and to reach a higher temperature.[12] Therefore, some volatiles of raw bamboo and masson pine blends with higher moisture content were not oxidized during this stage, especially for organic substances. This resulted in increasing of smoke. Figure 3a shows that bamboo had the highest TSP. TSP also increased with the bamboo content in blends, except for the blends of 40% bamboo and 60% masson pine. It was very interesting that torrefied bamboo had the lowest TSP, as shown in Figure 3b. This indicated that torrefaction could significantly decrease the TSP of bamboo. The TSP of torrefied blends was between bamboo and masson pine. But the effect of blend ratios on TSP was irregular. The smoke release of the torrefied biomass was faster to reach a steady stage, compared with the raw biomass. This phenomenon was also because of the removal of some combustible substance during the torrefaction process, resulting in a stable combustion process.

The release of CO and CO_2 were determined by cone calorimetry. Figure 4a,b shows CO emission during the cofiring process. There were two shoulder peaks with a similar trend. The CO release at the first stage was because of a decarboxylation reaction of the alkyl side chain of the carbonyl functional group (−CHO) contained in bamboo and masson pine.[18,19] The release amount of CO slightly increased with the increase of bamboo content in the blends. However, the CO release of torrefied masson pine and bamboo blends remained at a stable level at different blend ratios. This was mainly because of the pyrolysis of volatiles in the samples during the torrefaction process, which decreased the amount of −CHO. It was found that the main release of CO occurred at the second stage, which was caused by the increase of temperature and secondary reactions. Figure 4a shows that the peak corresponding to maximum CO release occurred at 150 s, which was significantly higher than that at the first stage. Figure 4b shows that the peak of maximum CO release began at 50 s for torrefied bamboo and masson pine blends, which was obviously sooner than that of raw biomass blends. This phenomenon was mainly caused by a longer char burn process when torrefied masson pine and bamboo blends burned. Based on the results of this research, the effect of torrefaction on CO release was not significant. CO_2 is also a major component of greenhouse gases, which has a significant impact on the environmental climate change. Figure 4c,d shows the emission of CO_2 from the cofiring process of raw/torrefied masson pine and bamboo blends. Raw masson pine and bamboo blends had two peaks of CO_2 emission, located at a range of 0−50 and 72−100 s. Compared with CO release, the first peak was the main CO_2 release. This confirmed that the CO_2 emission was from the combustion of volatiles. The second release peak was because of thermal cracking of the solid residue in the fuels, oxidation of biochar, and high temperature thermal decomposition. However, there was only one peak of CO_2 emission for torrefied masson pine and bamboo blends and its release amount was significantly lower than raw biomass blends. It was because of the decrease in the oxygen content of biomass after torrefaction.[20] Furthermore, there was no significant variation in the amount of CO_2 released at different blend ratios. It was interesting that CO_2 release curve was similar with the HRR curve, indicating that the heat release process was coincided with CO_2 release. It is well known that the mass loss of bamboo and masson pine is mainly because of the oxidation of carbon into CO_2 and the conversion of hydrogen and oxygen into water. Therefore, the dehydration reaction during the cofiring process of torrefied biomass blends was more than that

DOI: 10.1021/acsomega.9b02593
ACS Omega 2019, 4, 19246−19254

Table 2. Chemical Compositions of Ash Samples

chemical compositions (%)	masson pine (M)	20B:80M	40B:60M	60B:40M	80B:20M	bamboo (B)
MgO	4.98	9.19	10.9	11.8	13.2	14.2
Al_2O_3	8.53	4.22	2.26	1.66	1.09	0.767
SiO_2	21.8	16.1	15.4	17.6	18.6	19.7
P_2O_5	2.31	3.10	3.85	4.22	4.62	5.09
SO_3	3.79	5.38	6.71	7.40	7.70	7.97
K_2O	9.84	21.2	29.0	34.0	38.2	41.7
CaO	31.5	29.0	24.8	17.9	11.4	5.64
MnO	2.29	2.33	2.41	2.24	1.89	2.03
Fe_2O_3	11.1	6.02	3.07	1.66	1.28	0.781
ZnO	0.329	0.304	0.313	0.338	0.344	0.310
TiO_2	1.71	0.738	0.278	0.213	0.181	0.209
Cl	0.126	0.332	0.461	0.749	0.825	1.20

Table 3. Ash Fusion Indexes of all the Samples

indexes	masson pine (M)	20B:80M	40B:60M	60B:40M	80B:20M	bamboo (B)
R_A (%)	32.040	21.058	17.938	19.473	19.871	20.676
R_B (%)	57.420	66.198	67.770	65.360	64.080	62.321
[a] $R_{B/A}$	1.792	3.144	3.778	3.356	3.225	3.014
[b] $R_{B/A+P}$	1.864	3.291	3.993	3.573	3.457	3.260
[c] F_u	17.633	69.130	109.562	114.104	123.195	125.684
[d] λ (W/m K)	0.882	1.058	1.138	1.101	1.089	1.043
[e] S_R	31.421	26.695	28.429	35.948	41.817	48.858
AI	3.028	6.249	8.099	8.573	12.316	19.401

[a]Base to acid: $R_{B/A} = R_B/R_A = (Fe_2O_3 + CaO + MgO + Na_2O + K_2O)/(SiO_2 + Al_2O_3 + TiO_2)$. [b]Base to acid: $R_{B/A+P} = (Fe_2O_3 + CaO + MgO + Na_2O + K_2O + P_2O_5)/(SiO_2 + Al_2O_3 + TiO_2)$. [c]Fouling index: $F_u = R_{B/A}(Na_2O + K_2O)$. [d]Thermal conductivity: $\lambda = 0.773 \lg R_{B/A+P} + 0.673$. [e]Slag viscosity index: $S_R = SiO_2 \times 100/(SiO_2 + Fe_2O_3 + CaO + MgO)$.

of raw biomass blends according to the significant reduction in CO_2 release from torrefied biomass blends. In conclusion, the lower release of CO_2 and CO from torrefied blends indicated that torrefied bamboo and masson pine blends were environmentally friendly energy resources. Especially, blend ratios had not a significant impact on CO and CO_2 emissions of torrefied biomass blends, compared with raw biomass blends.

2.3. Ash Characteristics. *2.3.1. Chemical Compositions of Ash Samples.* Table 2 summarizes the chemical composition of ash samples. The major components were CaO (31.5%), SiO_2 (21.8%), Fe_2O_3 (11.1%), K_2O (9.84%), and Al_2O_3 (8.53%) in the ash of masson pine, whose contents were more than 80% of total ash. There were also other components, such as MgO (4.98%), SO_3 (3.79%), P_2O_5 (2.31%), and MnO (2.29%). However, bamboo ash was mainly composed of K_2O (41.7%), SiO_2 (19.7%), MgO (14.2%), and SO_3 (7.97%), whose contents were also more than 80% of total ash. It also included CaO (5.64%), P_2O_5 (5.09%), and MnO (2.03%). It was confirmed that the dominating elements in the slag were silicon, potassium, calcium, and magnesium during the cofiring of bamboo and masson pine. Although the main type of chemical compositions in the ash of bamboo or masson pine were similar, the contents was obviously different. The content of K_2O, MgO, and SO_3 in bamboo ash was significantly higher than that of masson pine ash. In contrast, bamboo ash had a lower content of CaO, Al_2O_3, and Fe_2O_3. For the ash of blends, the content of all major chemical compositions was between bamboo and masson pine. The percentage of MgO, P_2O_5, SO_3, K_2O, and Cl in the ash of blends gradually increased, whereas the content of Al_2O_3, CaO, and Fe_2O_3 gradually decreased with increase in the bamboo content of blends. It's worth noting that the SiO_2 content was the only species that did not behave linearly with the changing blend ratio. Alao it exhibited the lowest percentage with a value of 15.4% in the blend of 40% bamboo and 60% masson pine. This was a key factor to be taken into account when analyzing the characteristics of ash fusion. Chlorine (Cl) is also a non-negligible component during the combustion of the biomass fuel. It usually existed in the form of KCl or NaCl, which was a pivotal inorganic element to promote the release of K and accelerated the rate of corrosion and ash deposition.[21,22] Table 2 shows that the ash of bamboo had a slightly higher content of Cl than masson pine. The content of Cl gradually increased with increase in bamboo content of the blends. Among the chemical compositions of all the ash samples, there were three types of oxides. The acid oxides included SiO_2, P_2O_5, and TiO_2. The higher concentration of acid oxides with a high ionic potential (Si^{4+} is 95.24 nm^{-1}) was easy to form the low-melting temperature products.[23,24] The basic oxides included Na_2O, K_2O, MgO, CaO, and MnO_2, which could react with SiO_2 and Al_2O_3 to form low-MP alumino-silicate minerals.[25] Al_2O_3 and Fe_2O_3 were classified as amphoteric oxides. But Al_2O_3 was sometimes classified as an acidic oxide and Fe_2O_3 as a basic oxide. These chemical compositions affected ash fusion characteristics.

Table 3 shows ash fusion indexes, which had been widely used as reliable decisions for fusion tendency.[24,26] Wang et al.[27] concluded that all the ash samples represented a trend of high possibility of melting and fusion if $R_{B/A}$ was more than 0.7, F_u was more than 40, S_R was lower than 65, and AI was more than 0.34. The base-to-acid ratio ($R_{B/A+P}$ of 3.260 and $R_{B/A}$ of 3.014) of bamboo ash was higher than that of masson pine ($R_{B/A+P}$ of 1.864 and $R_{B/A}$ of 1.792). This phenomenon was attributed to the higher content of K_2O and MgO and the

DOI: 10.1021/acsomega.9b02593
ACS Omega 2019, 4, 19246−19254

lower content of Al_2O_3 and TiO_2 in bamboo ash. The value of $R_{B/A+P}$ or $R_{B/A}$ is commonly used to forecast the tendency of fouling tendencies of ash. The AFT included initial deformation temperature (DT), softening temperature (ST), hemispherical temperature (HT), and flow temperature (FT). DT was extensively deemed as an important index to evaluate ash fusion characteristics of biomass ash.[28,29] Figure 5 shows

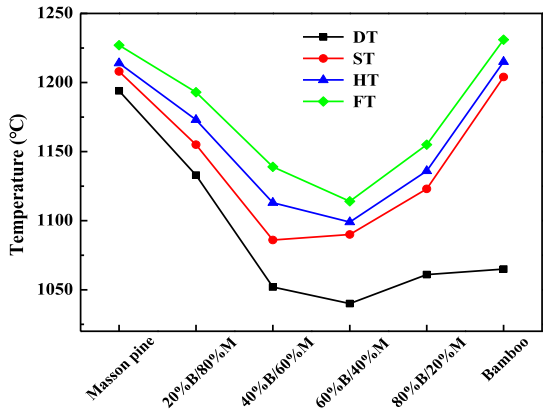

Figure 5. AFTs of all the ash samples with different blend ratios.

AFT of all the ash samples. The DT of masson pine ash (1194 °C) was higher than that of bamboo ash (1065 °C). The variation of chemical compositions was ascribed to this phenomenon. Even though the aluminum content (0.767%) was low in bamboo ash, the alkali metal and alkaline earth metal were high, such as K_2O, CaO, and MgO. Their total content was more than 60% of the total ash, which resulted in a decrease in AFT. This was mainly due to the fact that these high content of substances changed the stable network from tecto-silicates, ino-silicates, cyclo-silicates, and soro-silicates to neso-silicates.[25] Furthermore, most of the phosphorus in biomass ash existed in the form of phytic acid or phytate, which could be converted to K-phosphates, Mg-phosphates, K−Mg-phosphates, and phosphorus oxides.[30] These P-rich substances also resulted in a decrease in the AFT, which was closely associated with high sintering and slagging tendencies of ash.[31] Wang et al.[32] concluded that an increase in P_2O_5 promoted the formation of the low melting phase in the ash. This also resulted in a lower DT of bamboo ash than masson pine ash (P_2O_5 in bamboo and masson pine ash were, respectively, 5.09 and 2.31%). It was found that the ST, HT, and FT of bamboo and masson pine ash were relatively close. For the blends, the DT, ST, HT, and FT of blend ashes gradually decreased when the bamboo content of the blends increased from 0 to 60%. Then, they increased with increase in the bamboo content of the blends from 60 to 100%. The fusion temperatures of blend ashes were, respectively, lower than that of bamboo or masson pine ash, confirming that there was a synergistic reaction of ash component during the cofiring process of bamboo and masson pine.

2.3.2. Ash Surface Morphology. Ash fusion characteristics could be reflected by its surface morphology.[33] The surface morphology of the ashes determined by SEM and TEM are shown in Figures 6 and 7. It was found that the surface morphology of the ashes significantly varied with the change of bamboo content in the blends. Figure 6a−f shows the surface morphology of masson pine and bamboo ash, respectively. The ash of masson pine included many irregular snowflake particles (1−200 μm), which were evenly distributed on the surface of ash. In contrast, there was a less amount of aggregation on the surface of the bamboo ash. The pores from the shrinkage of the fiber structure during the release of the volatile matter resulted in these irregular microstructures.[34] When less amount of bamboo was mixed with masson pine, some small particle ashes gradually agglomerated and formed large particles with partially smooth and rough surfaces (Figure 6b). With increase in bamboo content of the blends, the aggregation on the surface of ash particles became more and more evident and some white molten mineral particles began to appear on larger particle molten surfaces (Figure 6c,d). This might be ascribed to the loss of the original fiber structure of the raw material, the rapid combustion of combustible elements, and the rapid shrinkage of the raw materials, which eventually melted and blocked the interior. With increase in the bamboo content, the phenomenon of surface aggregation slowed down and the distribution loosened (Figure 6e). It was concluded that the change of surface morphology of the blend ashes with different

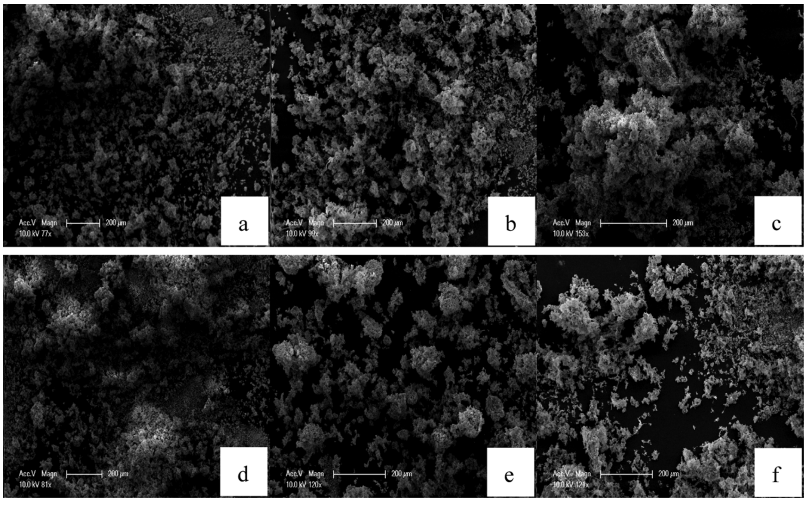

Figure 6. SEM of all the ash samples with different blend ratios (a) masson pine; (b) 20B:80M; (c) 40B:60M; (d) 60B:40M; (e) 80B:20M; and (f) bamboo.

DOI: 10.1021/acsomega.9b02593
ACS Omega 2019, 4, 19246−19254

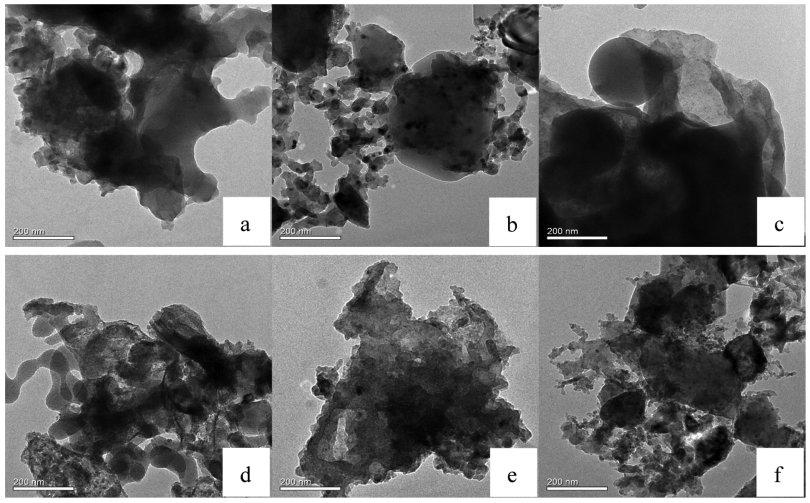

Figure 7. TEM of all the ash samples with different blend ratios (a) masson pine; (b) 20B:80M; (c) 40B:60M; (d) 60B:40M; (e) 80B:20M; and (f) bamboo.

blend ratios was consistent with the variation in its fusion temperature.

Compared with SEM, the morphology, surface texture, internal structure, and higher resolution information of ash can also be further expressed by TEM. The images (Figure 7) showed a variety of particle sizes (1−200 nm) with irregular shapes and predominantly round outlines (Figure 7b−d). The presence of round ash particles was due to the fact that they were produced by the agglomeration of evaporating substances, especially those containing S as it is a volatile element.[35] And it was also indicated that the minerals in the ash required a higher temperature to reach a melting state. There were aggregates of fine particles in some places on the ash surface, which resulted in densification of the ash sample. This phenomenon was mainly because of the high temperatures during repeated regeneration.

3. CONCLUSIONS

In summary, the present study demonstrated the further potential of using bamboo and masson pine residues as energy products. Torrefaction improved the fuel properties and converted bamboo or masson pine from a nonuniformity to a homogenous solid fuel, resulting in a more stable combustion process of the samples. Furthermore, torrefaction deceased in the release of HHR, THR, TSP, CO, and CO_2. Torrefied bamboo and masson pine blends were environmentally friendly energy resources. The chemical composition of bamboo and masson pine ash affected its fusion characteristics. Bamboo ash was easier to occur slagging, agglomeration or corrosion than that of masson pine. There was a synergistic reaction of ash components during the cofiring process. The ash sample of 60% bamboo and 40% masson pine had the lowest initial DT.

4. EXPERIMENTAL SECTION

4.1. Materials. Moso bamboo (*Phyllostachys heterocycla*) and masson pine (*Pinus massoniana* Lamb.) were used in this study. Moso bamboo aged 4 years old was taken from a bamboo plantation located in Zhejiang Province, China. The initial moisture content was about 6.45%. Masson pine aged 20 years old was taken from Anhui Province, China. The initial moisture content was about 10%. They were broken down to particles using a Wiley Mill. Samples were screened to get 250−425 μm particles, which were dried at temperature 105 °C for 24 h. Bamboo and masson pine particles were torrefied at a temperature of 300 °C for 2 h with a heating rate of 5 °C/min in a muffle furnace under a nitrogen atmosphere.[36] Raw and torrefied bamboo or masson pine were, respectively, mixed with mass ratios of 20:80, 40:60, 60:40, and 80:20.

4.2. Determination of Proximate and Ultimate. The determination of moisture and volatiles was performed according to GB/T 212-2008. The determination of inorganic ash was performed according to D1102-84. The determination of the high heating value was performed according to ASTM E 711. The determination of C, H, and N was performed according to GB/T 476-2008. The oxygen content was obtained by difference.

4.3. Determination of Combustion Characteristics. Combustion characteristics of the samples including HRR, THR, TSP, CO, and CO_2 production were determined using a cone calorimeter (Fire Testing Technology LTD., UK) with a heat flux of 50 kW/m^2 based on the ISO 5660-1 standard. The samples were evenly put into a mold with 100 mm (long) × 100 mm (wide) × 8 mm (thickness). The tests were carried out at a horizontal orientation. Three replicates of each experiment were performed.

4.4. Determination of Ash Characteristics. The ash samples were prepared using a digitally controlled GSL 1600X tube furnace according to the standard method of GB/T 28731-2012.

(1) The main chemical composition of all the ash samples was determined by an XRF spectrometer, produced by Shimadzu in Japan. Three replicates of each experiment were performed.

(2) The surface morphology of ashes was determined by an XL30 ESEM-FEG Scanning Electron Microscope. TEM measurement was conducted with a high resolution Tecnai G220, operating at 200 kV and room temperature.

(3) The fusion temperatures (AFTs) of all the ash samples were carried out according to the standard method (GB/T 30726-2014) by a YX-HRD testing instrument. Four characteristic temperatures of ash including DT, ST, HT, and FT were determined based on the ash cone calorimeters with a video camera and recorded

DOI: 10.1021/acsomega.9b02593
ACS Omega 2019, 4, 19246−19254

automatically with the accuracy of 1 °C. The determination of the samples was conducted under the weak reduction atmosphere.

AUTHOR INFORMATION

Corresponding Author

*E-mail: Liuzj@icbr.ac.cn. Phone: 86-10-84789869 (Z.L.).

ORCID

Hongzhong Xiang: 0000-0003-4905-4635

Notes

The authors declare no competing financial interest.

ACKNOWLEDGMENTS

This research was financially supported by the "Basic Scientific Research Funds of International Centre for Bamboo and Rattan-Manufacturing Technology of Biochar from Mixture of Bamboo and Wood"(grant no. 1632018020) and the "13th Five Years Plan-Study on Manufacturing Technology of Bamboo Wastes and its Mechanism" (grant no. 2016YFD0600906).

NOMENCLATURE

AI	alkali index
B	bamboo
C	carbon
DT	deformation temperature (°C)
FC	fixed carbon
FT	flow temperature (°C)
F_u	fouling index
H	hydrogen
HHV	higher heating value (MJ/kg)
HRR	heat release rate (kW/m^2)
HT	hemispherical temperature (°C)
M	masson pine
N	nitrogen
O	oxygen
PHRR	peak heat release rate (kW/m^2)
$R_{B/A}$	base to acid (no P_2O_5)
$R_{B/A+P}$	base to acid (contains P_2O_5)
S	sulphur
S_R	slag viscosity index
ST	softening temperature (°C)
SEM	scanning electron microscopy
THR	total heat release (kJ/m^2)
TSP	total suspended particulates (m^2)
TEM	transmission electron microscopy
VM	volatile matter
XRF	X-ray fluorescence
YX-HRD	YX-HRD testing instrument

Greek Letters

λ	thermal conductivity

REFERENCES

(1) Wang, G.; Zhang, J.; Shao, J.; Liu, Z.; Zhang, G.; Xu, T.; Guo, J.; Wang, H.; Xu, R.; Lin, H. Thermal behavior and kinetic analysis of co-combustion of waste biomass/low rank coal blends. *Energy Convers. Manage.* **2016**, *124*, 414−426.

(2) Barmina, I.; Valdmanis, R.; Zake, M. The effects of biomass co-gasification and cofiring on the development of combustion dynamics. *Energy* **2018**, *146*, 4−12.

(3) Tokarski, S.; Głód, K.; Śoódrsk, M.; Zuwała, J. Comparative assessment of the energy effects of biomass combustion and cofiring in selected technologies. *Energy* **2015**, *92*, 24−32.

(4) Wang, X.; Ren, Q.; Li, L.; Li, S.; Lu, Q. TG−MS analysis of nitrogen transformation during combustion of biomass with municipal sewage sludge. *J. Therm. Anal. Calorim.* **2016**, *123*, 2061−2068.

(5) Kwong, P. C. W.; Chao, C. Y. H.; Wang, J. H.; Cheung, C. W.; Kendall, G. Co-combustion performance of coal with rice husks and bamboo. *Atmos. Environ.* **2007**, *41*, 7462−7472.

(6) Rousset, P.; Aguiar, C.; Labbé, N.; Commandré, J.-M. Enhancing the combustible properties of bamboo by torrefaction. *Bioresour. Technol.* **2011**, *102*, 8225−8231.

(7) Bada, S. O.; Falcon, R. M. S.; Falcon, L. M. Investigation of combustion and co-combustion characteristics of raw and thermal treated bamboo with thermal gravimetric analysis. *Thermochim. Acta* **2014**, *589*, 207−214.

(8) Liu, Z.; Hu, W.; Jiang, Z.; Mi, B.; Fei, B. Investigating combustion behaviors of bamboo, torrefied bamboo, coal and their respective blends by thermogravimetric analysis. *Renewable Energy* **2016**, *87*, 346−352.

(9) Mi, B.; Liu, Z.; Hu, W.; Wei, P.; Jiang, Z.; Fei, B. Investigating pyrolysis and combustion characteristics of torrefied bamboo, torrefied wood and their blends. *Bioresour. Technol.* **2016**, *209*, 50−55.

(10) Leonelli, L.; Barboni, T.; Santoni, P. A.; Quilichini, Y.; Coppalle, A. Characterization of aerosols emissions from the combustion of dead shrub twigs and leaves using a cone calorimeter. *Fire Saf. J.* **2017**, *91*, 800−810.

(11) Chen, D.; Zhou, J.; Zhang, Q. Effects of Torrefaction on the Pyrolysis Behavior and Bio-Oil Properties of Rice Husk by Using TG-FTIR and Py-GC/MS. *Energy Fuels* **2014**, *28*, 5857−5863.

(12) Pimchuai, A.; Dutta, A.; Basu, P. Torrefaction of agriculture residue to enhance combustible properties. *Energy Fuels* **2010**, *24*, 4638−4645.

(13) Chen, W.-H.; Ye, S.-C.; Sheen, H.-K. Hydrothermal carbonization of sugarcane bagasse via wet torrefaction in association with microwave heating. *Bioresour. Technol.* **2012**, *118*, 195−203.

(14) Goldfarb, J. L.; Ceylan, S. Second-generation sustainability: Application of the distributed activation energy model to the pyrolysis of locally sourced biomass−coal blends for use in cofiring scenarios. *Fuel* **2015**, *160*, 297−308.

(15) Wang, M.; Wang, X.; Li, L.; Ji, H. Fire performance of plywood treated with ammonium polyphosphate and 4A zeolite. *BioResources* **2014**, *9*, 4934−4945.

(16) Fateh, T.; Rogaume, T.; Luche, J.; Richard, F.; Jabouille, F. Characterization of the thermal decomposition of two kinds of plywood with a cone calorimeter - FTIR apparatus. *J. Anal. Appl. Pyrolysis* **2014**, *107*, 87−100.

(17) Hellwig, G. Basic of the combustion of wood and straw. In *Energy from biomass, 3rd E.C. Conference*; Palz, W., Coombs, J., Hall, D. O., Eds.; Elsevier Applied Science: London, 1985; pp 793−798.

(18) Cao, J.; Xiao, G.; Xu, X.; Shen, D.; Jin, B. Study on carbonization of lignin by TG-FTIR and high-temperature carbonization reactor. *Fuel Process. Technol.* **2013**, *106*, 41−47.

(19) Parshetti, G. K.; Liu, Z.; Jain, A.; Srinivasan, M. P.; Balasubramanian, R. Hydrothermal carbonization of sewage sludge for energy production with coal. *Fuel* **2013**, *111*, 201−210.

(20) Chen, Y.; Yang, H.; Yang, Q.; Hao, H.; Zhu, B.; Chen, H. Torrefaction of agriculture straws and its application on biomass pyrolysis poly-generation. *Bioresour. Technol.* **2014**, *156*, 70−77.

(21) Johansen, J. M.; Aho, M.; Paakkinen, K.; Taipale, R.; Egsgaard, H.; Jakobsen, J. G.; Frandsen, F. J.; Glarborg, P. Release of K, Cl, and S during combustion and co-combustion with wood of high-chlorine biomass in bench and pilot scale fuel beds. *Proc. Combust. Inst.* **2013**, *34*, 2363−2372.

(22) Li, Y. S.; Spiegel, M.; Shimada, S. Corrosion behaviour of various model alloys with NaCl−KCl coating. *Mater. Chem. Phys.* **2005**, *93*, 217−223.

DOI: 10.1021/acsomega.9b02593
ACS Omega 2019, 4, 19246−19254

(23) Nel, M. V.; Strydom, C. A.; Schobert, H. H.; Beukes, J. P.; Bunt, J. R. Reducing atmosphere ash fusion temperatures of a mixture of coal-associated minerals - the effect of inorganic additives and ashing temperature. *Fuel Process. Technol.* **2014**, *124*, 78−86.
(24) Magdziarz, A.; Dalai, A. K.; Koziński, J. A. Chemical composition, character and reactivity of renewable fuel ashes. *Fuel* **2016**, *176*, 135−145.
(25) Ma, X.; Li, F.; Ma, M.; Fang, Y. Investigation on blended ash fusibility characteristics of biomass and coal with high silica-alumina. *Energy Fuels* **2017**, *31*, 7941−7951.
(26) Pronobis, M. Evaluation of the influence of biomass co-combustion on boiler furnace slagging by means of fusibility correlations. *Biomass Bioenergy* **2005**, *28*, 375−383.
(27) Wang, L.; Skjevrak, G.; Skreiberg, Ø.; Wu, H.; Nielsen, H. K.; Hustad, J. E. Investigation on ash slagging characteristics during combustion of biomass pellets and effect of additives. *Energy Fuels* **2018**, *32*, 4442−4452.
(28) Niu, Y.; Tan, H.; Wang, X.; Liu, Z.; Liu, H.; Liu, Y.; Xu, T. Study on fusion characteristics of biomass ash. *Bioresour. Technol.* **2010**, *101*, 9373−9381.
(29) Niu, Y.; Du, W.; Tan, H.; Xu, W.; Liu, Y.; Xiong, Y.; Hui, S. Further study on biomass ash characteristics at elevated ashing temperatures: the evolution of K, Cl, S and the ash fusion characteristics. *Bioresour. Technol.* **2013**, *129*, 642−645.
(30) Wang, Q.; Han, K.; Gao, J.; Wang, J.; Lu, C. Investigation of maize straw char briquette ash fusion characteristics and the influence of phosphorus additives. *Energy Fuels* **2017**, *31*, 2822−2830.
(31) Lindström, E.; Sandström, M.; Boström, D.; Öhman, M. Slagging characteristics during combustion of cereal grains rich in phosphorus. *Energy Fuels* **2007**, *21*, 710−717.
(32) Wang, L.; Skjevrak, G.; Hustad, J. E.; Grønli, M. G. Sintering characteristics of sewage sludge ashes at elevated temperatures. *Fuel Process. Technol.* **2012**, *96*, 88−97.
(33) Li, F.; Xu, M.; Wang, T.; Fang, Y.; Ma, M. An investigation on the fusibility characteristics of low-rank coals and biomass mixtures. *Fuel* **2015**, *158*, 884−890.
(34) Ren, X.; Sun, R.; Meng, X.; Vorobiev, N.; Schiemann, M.; Levendis, Y. A. Carbon, sulfur and nitrogen oxide emissions from combustion of pulverized raw and torrefied biomass. *Fuel* **2017**, *188*, 310−323.
(35) Buhre, B. J. P.; Hinkley, J. T.; Gupta, R. P.; Wall, T. F.; Nelson, P. F. Submicron ash formation from coal combustion. *Fuel* **2005**, *84*, 1206−1214.
(36) Liu, Z.; Fei, B.; Jiang, Z.; Liu, X. E. Combustion characteristics of bamboo-biochars. *Bioresour. Technol.* **2014**, *167*, 94−99.

DOI: 10.1021/acsomega.9b02593
ACS Omega 2019, 4, 19246−19254